Electronic Supplementary Information (ESI)

Hidden gapless states during thermal transformations of preorganized zinc alkoxides to zinc oxide nanocrystals

Jakub Szlachetko,[a,b] Adam Kubas,[b] Anna Maria Cieślak,[b] Kamil Sokołowski,[b] Łukasz Mąkolski,[c] Joanna Czapla-Masztafiak,[a] Jacinto Sá,[a,d]* Janusz Lewiński[a,c]*

[a.] *Institute of Physical Chemistry Polish Academy of Sciences Kasprzaka 44/52, 01-224 Warsaw, Poland*

[b.] *Institute of Nuclear Physics Polish Academy of Sciences Radzikowskiego 152, 31-342 Kraków, Poland*

[c.] *Faculty of Chemistry Warsaw University of Technology Noakowskiego 3, 00-664 Warsaw, Poland*

[d.] *Physical Chemistry Division, Departament of Chemistry, Ångström Laboratory, Uppsala University, Lägerhyddsvägen 1, 75120 Uppsala, Sweden*

Table of Contents

Experimental Procedures

Synthesis

[*t*BuZn(μ_3-O*t*Bu)]$_4$ (**1**) was synthetized according to the procedure described previously.[1] Shortly, Zn*t*Bu$_2$ (0.718 g, 4.00 mmol) in toluene (4 mL) was added dropwise to a solution of *t*BuOH (0.296 g, 4.00 mmol) in toluene (4 mL) at –78°C. After the addition was completed the reaction mixture was allowed to warm to RT and stirred for further 2h. [*t*BuZn(μ_3-O*t*Bu)]$_4$ was obtained as colorless rhomboidal crystals after crystallization from toluene/hexane mixture at 4°C; isolated yield ca. 84 %. Elemental analysis (%) calcd for C32H72O4Zn4: C 49.12, H 9.28; found: C 49.04, H 9.40; ^{1}H NMR (toluene-*d*8, 400.10 MHz, 298 K): δ = 1.32 (s, 9H, OC(C*H3)*3), 1.30 (s, 9H, ZnC(C*H3)*3) ppm.

X-ray spectroscopy study

We applied v2c-XES and HEROS (Fig. 1A) techniques to reveal occupied and unoccupied electronic states around the Fermi level. The high-energy resolution, necessary for detailed spectral measurements, was provided by dispersive-type spectrometer arranged in von Hamos geometry and schematically shown in Fig. 1B.[2] The spectrometer allows measuring wide range of X-ray spectra without necessity of moving or scanning spectrometer's component. Due to this, high-energy resolution measurements are performed at short acquisition times that are crucial to follow changes in electronic structure of transforming material. Schematic of the v2c-XES process is drawn in Fig. 1A, left. In this case, the incidence X-ray energy is set far above ionization threshold. As a result of photo-absorption event, the core-electron is ejected from an atom leading to creation of deep lying core-hole state. This state decays then radiatively by electronic transition from higher electron-occupied orbitals. Therefore, the valence states occupancy can be determined by measuring the X-ray emission spectra that corresponds to transition form highest occupied electronic states onto the core-hole.[3]

The method of high-energy resolution off-resonant spectroscopy relies on measuring the unoccupied electronic states above Fermi level at fixed incidence X-ray energy that is set below an ionization threshold.[8a,d,4] In such regime, the absorption of X-ray by core-electron leads to virtual intermediate state. Within the core-hole lifetime, the excited electron probes unoccupied electronic states with probability defined as 1/E (as schematically shown in Fig. 1A), where E is the energy of excited electron. This intermediate excited state decays radiatively and, through the energy conversation principle, the energy of emitted X-ray depend on the energy of excited electron. Thanks to this correspondence, the off-resonant X-ray emission spectrum reflects density of unoccupied states of scattering atom at fixed incidence X-ray energy. Importantly, both v2c-XES and HEROS spectroscopies will provide projected density of states being defined by the orbital angular momentum of core-excited electron. Thus, depending on absorption edge (core-hole state) employed in the experiment the partial occupied and unoccupied electronic states are investigated.

The experiment was conducted at SuperXAS beamline of Swiss Light Source, Switzerland. The spectra were measured around K-absorption edge of Zn at 9659 eV. The X-rays were delivered by bending magnet and collimated by means of Si mirror working at 3mRad incidence angle and monochromatized with double Si(111) crystals. Downstream the monochromator we used toroid-shape Pt-coated mirror for X-ray focusing. At sample position the X-ray size was 100 x 100 μm^2 with X-ray flux of 5x10^{11} photons/s. For X-ray detection we employed von Hamos spectrometer arranged in vertical scattering geometry.[10] For measurements of Kβ-HEROS and v2c-XES signals a Ge(800) X-ray diffraction crystal was employed that provides central Bragg angle of 65°. The crystal was glued to aluminum support with curvature radius of 250mm. The X-rays diffracted by the crystal were recorded with Pilatus 2D detector having pitch size of 172 μm. The experimental resolution of 1.5 eV was determined from elastic scattering peak measurements and found to be comparable to the Zn *1s* core-hole lifetime of 1.62 eV. The same elastic peak measurements were used for X-ray spectrometer calibration. A two incidence X-ray energies were used to measure v2c and off-resonant X-ray emission signals. For v2c spectroscopy incidence X-ray energy of 9715 eV was used that is about 50 eV above the ionization threshold. During HEROS experiment the incidence energy was detuned by 10eV below ionization threshold.

The [*t*BuZn(μ_3-O*t*Bu)]$_4$ sample in form of powder was enclosed in quartz capillary with connected inlet and outlet gas tubes and kept under Ar environment. The temperature was controlled with air-blower located under capillary, and experiment was performed with temperature ramping of 10 °C/min in the range between 20 and 500 °C. Temperature at sample position was calculated as average temperature measured before and after capillary by means of pair of thermocouples. During temperature decomposition the experimental spectra were measured with acquisition time of 30 s per one data point.

High Resolution Transmition Electron Microscopy

Samples for HRTEM were prepared by drop casting of an THF suspension of the ZnO NCs, obtained as a final product of the v2c-XES and HEROS experiments, onto 300-mesh, holey carbon-coated copper grids (Quantifoil). The characterization of size, shape and morphology was carried out on a high resolution Scanning Transmission Electron Microscope (FEI TECNAI G2 F20 S-TWIN; Institute of High Pressure Physics of the Polish Academy of Sciences) with the following optical parameters: C_S = 1.2 mm, C_c = 1.2 mm, electron energy spread = 0.7 eV, beam divergence semi-angle = 1 mrad. Particle size distributions were calculated by counting the diameters of more than 100 particles.

Thermogravimetric analysis

Thermogravimetric analysis (TGA) was performed in a dry argon atmosphere using open alumina crucibles on a TA Instruments Q600 simultaneous TG-DSC analyzer. The experiment was performed for the heating scheme corresponding to X-ray spectroscopy studies with temperature ramping of 10 °C/min in the range between 20 and 500 °C. Temperature was equilibrated for 30s in points corresponding to temperatures in which v2c-XES and HEROS data points where collected.

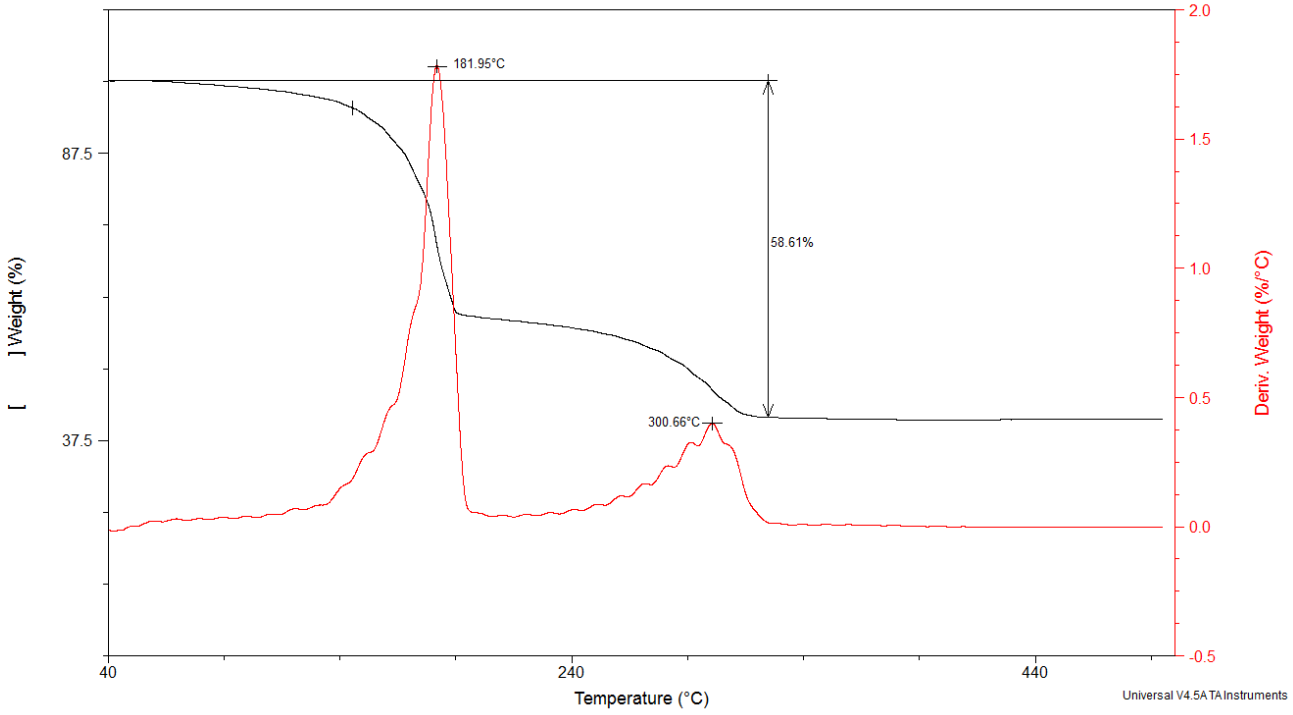

Figure S1. Thermogravimetric analysis of single source precursor **1** under heating scheme corresponding to X-ray spectroscopy studies. We note, that in this study the decomposition of **1** is completed around 300°C, which is shifted ca. 60°C towards higher temperatures in comparison to our previous TGA studies for **1** where 2°C/min heating rate was applied and the decomposition was finished around 240°C.[5]

Quantum chemical calculations

The calculations were performed using ORCA 3.0.3[6] program package using BP86[7a-e] generalized-gradient approximation functional for geometry optimizations and frequency calculations. Final single-point energies were calculated with the hybrid B3LYP[6,8a-b] functional on the top of BP86-optimised geometries. Both functionals were augmented with the most recent D3 pairwise correction for dispersion interactions along with the Becke-Johnson damping function.[9a-b] We took the advantage of the resolution of identity (RI) approximation for Coulomb terms[10a-b] while the exchange integrals were efficiently evaluated with the 'chain-of-spheres' approximation (RIJCOSX).[11a-b] The computations utilized triple-ζ quality all-electron def2-TZVP[12a-b] basis set along with the corresponding Coulomb-fitting auxiliary basis set def2-TZVP/J.[13] We used enlarged grid for numerical integrations denoted as

'grid4' in the ORCA nomenclature. RIJCOSX integration grid was set to 'gridx5'. All stationary geometries were subject to analytical second derivative calculations and no imaginary frequencies were identified in all structures. Frequencies above 50 cm^{-1} were used to obtain correction for enthalpy (H; includes ZPE and thermal corrections at 298.15 K).

Excitation energies were calculated with the recently developed restricted open-shell configuration interaction singles (ROCIS)[14 a-b] method using restricted closed-shell or restricted open-shell Kohn-Sham reference orbitals for closed-shell or open-shell molecules, respectively. In such hybrid B3LYP/ROCIS scheme, Coulomb and exchange integrals need to be scaled down to avoid double counting of electron-electron interactions. For this purpose, we used scaling-parameters of c_1=0.18 and c_2=0.24 for these integrals, respectively. Based on our experience, such choice provides balanced description of closed- and open-shell compounds and a detailed benchmark will be published elsewhere.[15]

Zn-C vs Zn-O bond cleavage

The calculated gas-phase enthalpy of anticipated hemolytic Zn-C bond cleavage in **1**, leading to the formation of a transient radical [•Zn(μ_3-OR)][RZn(μ_3-OR)]$_3$ species (**I_A**), is positive ($\Delta H_{1\rightarrow 2}$ = 55.5 kcal/mol) but plausible in high-temperature process investigated in this study. We also note the increase in entropy upon alkyl radical release that is not covered in our calculations. In an alternative scenario, *tert*-butyl radicals can be initially formed by a homolytic O-C bond cleavage. However, such process is highly unlikely as it has much more positive change in enthalpy (76.1 kcal/mol) and thus is thermodynamically disfavored over Zn-C bond cleavage. Moreover, the dicubane **I_B** is most likely connected *via* single Zn-Zn bond that is preferred over Zn-O bond (see **Figure S2**). This is particularly due to steric encumbrances. We therefore suggest that the homolytic zinc-carbon bond cleavage initiate further radical chain transformations.

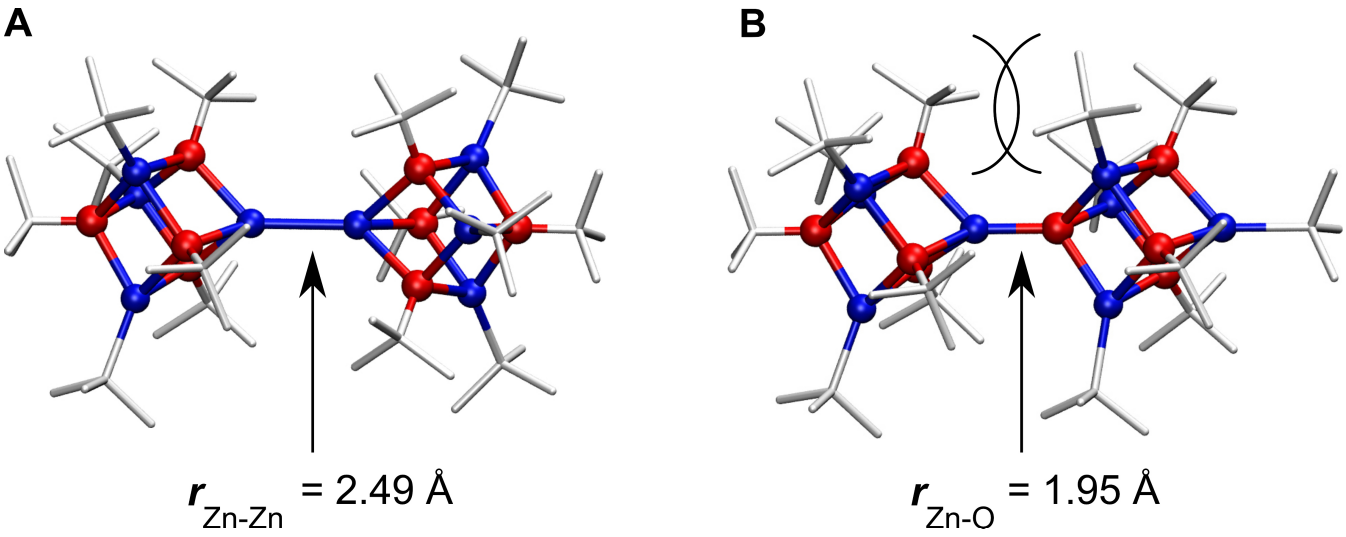

Figure S2. Structure of dicubanes connected by (A) Zn-Zn bond (structure **I_B** in the main text) and (B) by Zn-O bond. The latter is found to be higher in energy by 25.7 kcal/mol due to steric encumbrances between the alkyl groups (marked in panel B) caused by a short Zn-O distance of 1.95 Å as compared to relatively long Zn-Zn bond (2.51 Å).

Band-gap estimations from gas-phase calculations

First excitation energy (ΔE_{exc}) of the gas-phase structure can be considered as an approximation to a direct band-gap of the solid state especially when the transition has local HOMO-LUMO character. Another, rough way to track the changes of a band-gap is to look at HOMO-LUMO energy difference ($\Delta E_{HOMO\text{-}LUMO}$). The latter is unfortunately strongly dependent on the details of calculations as the one-electron energies ("orbital energies") obtained with different functionals vary quite strongly. However, to obtain complete picture **Table S1** provides both ΔE_{exc} and $\Delta E_{HOMO\text{-}LUMO}$ (calculated with B3LYP/ROCIS method and obtained with BP86 or B3LYP orbital energies, respectively) for all intermediates depicted in **Scheme 2** in the main text.

Table S1. BP86 and B3LYP HOMO-LUMO gaps ($\Delta E_{HOMO\text{-}LUMO}$) as well as B3LYP/ROCIS first excitation energies (ΔE_{exc}) of the species involved in the proposed [*t*BuZn(μ_3-O*t*Bu)]$_4$ decomposition path. Structures **III$_A$** and **III$_B$** represents bulk ZnO that is approximated with clusters of growing size $[ZnO]_4$ - $[ZnO]_8$. All values in eV.

	$\Delta E_{HOMO\text{-}LUMO}$		ΔE_{exc}
	BP86	B3LYP	
1	4.42	5.99	5.42
I$_A$	1.11*	2.29*	2.91
I$_B$	3.92	5.42	4.82
II$_A$	0.27*	1.27*	0.14
III$_A$ $[ZnO]_4$	1.69	3.30	2.60
III$_B$ $[ZnO]_8$	2.47	4.19	3.25

**LUMO(β)-HOMO(α) that is consistent with quasi-restricted orbitals (QROs) definition used in B3LYP/ROCIS calculations.*

From the experimental perspective, ΔE_{exc} can be used as a first approximation to the direct band-gap as the calculated numbers correspond to the experimental estimates. $\Delta E_{HOMO\text{-}LUMO}$ differences, in contrast, should be used carefully as they show similar trends in band-gap changes but absolute values may be far from experimental results. Moreover, we note some difficulty in defining $\Delta E_{HOMO\text{-}LUMO}$ gap in open-shell systems where two sets of orbitals are obtained in spin-unrestricted calculations. The gap will depend on whether it is calculated only between α-HOMO-LUMO, β-HOMO-LUMO or between HOMO(α) and LUMO(β). In our case we found latter definition to provide better correlation with B3LYP/ROCIS excitation energies particularly due to consistency with quasi-restricted orbitals (QROs) that are used to build the reference determinant in subsequent ROCIS calculations.

References

[1] J. Lewiński, M. Dutkiewicz, M. Lesiuk, W. Śliwiński, K. Zelga, I. Justyniak, J. Lipkowski, *Angew. Chem. Int. Ed* **2010**. ,*49*, 8266.

[2] J. Szlachetko, M. Nachtegaal, E. de Boni, M. Willimann, O. Safonova, J. Sá, G. Smolentsev, M. Szlachetko, J. A. van Bokhoven, J.-Cl. Dousse, J. Hoszowska, Y. Kayser, P. Jagodzinski, A. Bergamaschi, B. Schmitt, C. David, A. Lücke, *Rev. Sci. Instr.* **2012**, *83*, 103105.

[3] K. M. Lancaster, M. Roemelt, P. Ettenhuber, Y.Hu, M. W. Ribbe, F. Neese, U. Bergmann, S. DeBeer, *Science* **2011**, *334*, 974.

[4] W. Błachucki, J. Szlachetko, J. Hoszowska, J.-C. Dousse, Y. Kayser, M. Nachtegaal, J. Sá, *Phys. Rev. Lett.* **2014**, *112*, 173003.

[5] a) W. Bury, E. Krajewska, M. Dutkiewicz, K. Sokołowski, I. Justyniak, Z. Kaszkur, K. J. Kurzydłowski, T. Płociński and J. Lewiński, *Chem. Commun.,* **2011**, *47*, 5467; b) K. Sokołowski, I. Justyniak, W. Bury, J. Grzonka, Z. Kaszkur, Ł. Mąkolski, M. Dutkiewicz, A. Lewalska, D. Kubicki, K. Wójcik, K. Kurzydłowski and J. Lewiński, *Chem. Eur. J.,* **2015**, *21*, 5488.

[6] F. Neese, *Comp. Mol. Sci.* **2012**, *2*, 73.

[7] a) P. Dirac, *Proc. R. Soc. Lond. A* **1929**, *123*, 714; b) J. C. Slater, *Phys. Rev.* **1951**, *81*, 385; c) J. Perdew, *Phys. Rev. B* **1986**, *33*, 8822; d) A. D. Becke, *Phys. Rev. A,* **1988**, *38*, 3098; e) S. H. Vosko, L. Wilk, M. Nusair, *Can. J. Phys.* **1980**, *58*, 1200.

[8] a) C. Lee, W. Yang, R. G. Parr, *Phys. Rev. B* **1988**, *37*, 785; b) A. D. Becke, *J. Chem. Phys.* **1993**, *98*, 5648.

[9] a) S. Grimme, J. Antony, S. Ehrlich, H. Krieg, *J. Chem. Phys.* **2010**, *132*, 154104; b) S. Grimme, S. Ehrlich, L. Goerigk, *J. Chem. Phys.* **2011**, *32*, 1456.

[10] a) K. Eichkorn, O. Treutler, H. Öhm, M. Häser, R. Ahlrichs, *Chem. Phys. Lett.* **1995**, *240*, 283; b) M. Sierka, A. Hogekamp, R. Ahlrichs, *J. Chem. Phys.* **2003**, *118*, 9136.

[11] a) F. Neese, F. Wennmohs, A. Hansen, U. Becker, *Chem. Phys.* **2009**, *356*, 98; b) R. Izsák, F. Neese, *J. Chem. Phys.* **2011**, *135*, 144105.

[12] a) F. Weigend, M. Häser, H. Patzelt, R. Ahlrichs, *Chem. Phys. Lett.* **1998**, *294*, 143; b) F. Weigend, R. Ahlrichs, *Phys. Chem. Chem. Phys.* **2005**, *7*, 3297.

[13] F. Weigend, *Phys. Chem. Chem. Phys.* **2006**, *8*, 1057.

[14] a) M. Roemelt, F. Neese, *J. Phys. Chem. A* **2013**, *117*, 3069; b) M. Roemelt, D. Maganas, S. DeBeer, F. Neese, *J. Chem. Phys.* **2013**, *138*, 204101

Author Contributions

J.Sz., A.M.C., K.S., J.Sá, and J.L. conceived and supervised the experiments. A.M.C., K.S., and L.M. contributed to materials preparation. J.Sz. and J.Sá designed the XAS/XES experiments. J.Sz., A.M.C., J.C.-M., and J.Sá performed the XAS/XES experiments. A.K. designed and performed the theoretical calculations. J.Sz., A.K., K.S., J.Sá, and J.L. wrote the manuscript. All authors contributed to the discussion and reviewed the manuscript. All authors have given approval to the final version of the manuscript.